Generation of Synthetic SAS Data for Targets near the Seafloor: Propagation Component

Steven G. Kargl
Applied Physics Laboratory, University of Washington
1013 NE 40th St.
Seattle WA 98105-6698
Phone: (206) 685-4677 FAX: (206) 543-6785 Email: kargl@apl.washington.edu

Award Number: N00014-10-1-0114
http://www.apl.washington.edu/projects/projects.php/

LONG-TERM GOALS

The primary objective of the proposed research is continued development of an APL-UW synthetic aperture sonar simulation tool (SAS-ST). This tool can generate sets of realistic signals suitable for SAS and acoustic color template (i.e., target strength as a function of aspect angle and frequency) processing for targets near the seafloor. Updates to the propagation component are tested and validated against experimental data.

OBJECTIVES

The proposed research includes a few specific aims for improvements to SAS-ST. First, a fast ray-based model for propagation in a homogenous waveguide, which tracks time-of-flight wave packets from sources to targets and then to receivers, was reduced a fluid-fluid, half-space model and applied to a circular SAS simulation. The ray model use image sources and receivers to account for interaction with the water-sediment interface. Validation of the half-space model was carried out by comparison to Pond Experiment 2010 (PondEx10) data and against finite-element model (FEM) simulations.

APPROACH

A ray-base model developed in FY11 assumed a homogeneous layer water between an upper semi-infinite half-space of air and a lower semi-infinite half-space of a homogenous sediment. Rays are assumed to travel in straight line segments from a source location to a target location and after interacting with the target to a receiver location. For an interaction of a ray with an interface, an appropriate reflection coefficient is included in the contribution to the scattered signal. At present the sediment can be modeled as either an attenuating fluid with a frequency-independent loss parameter or a effective density fluid model. For the rays that interact with the interfaces, these rays can be represented as coming from image sources or arriving at image receivers. For a (image) source or (image) receiver located at $\boldsymbol{r}_i$ and a target located at $\boldsymbol{r}_t$, the horizontal and total separation distances are $|\boldsymbol{R}_i - \boldsymbol{R}_t|$ and $|\boldsymbol{r}_i - \boldsymbol{r}_t|$, respectively. The contribution of the ith source and the jth receiver to the frequency spectrum of the total scattered signal can be written as

Report Documentation Page

Form Approved
OMB No. 0704-0188

1. REPORT DATE	2. REPORT TYPE	3. DATES COVERED
2012	**N/A**	**-**

4. TITLE AND SUBTITLE	5a. CONTRACT NUMBER
Generation of Synthetic SAS Data for Targets near the Seafloor: Propagation Component	5b. GRANT NUMBER
	5c. PROGRAM ELEMENT NUMBER
6. AUTHOR(S)	5d. PROJECT NUMBER
	5e. TASK NUMBER
	5f. WORK UNIT NUMBER
7. PERFORMING ORGANIZATION NAME(S) AND ADDRESS(ES) **Applied Physics Laboratory, University of Washington 1013 NE 40th St. Seattle WA 98105-6698**	8. PERFORMING ORGANIZATION REPORT NUMBER
9. SPONSORING/MONITORING AGENCY NAME(S) AND ADDRESS(ES)	10. SPONSOR/MONITOR'S ACRONYM(S)
	11. SPONSOR/MONITOR'S REPORT NUMBER(S)

12. DISTRIBUTION/AVAILABILITY STATEMENT
Approved for public release, distribution unlimited

13. SUPPLEMENTARY NOTES
The original document contains color images.

14. ABSTRACT

15. SUBJECT TERMS

16. SECURITY CLASSIFICATION OF:			17. LIMITATION OF ABSTRACT	18. NUMBER OF PAGES	19a. NAME OF RESPONSIBLE PERSON
a. REPORT	b. ABSTRACT	c. THIS PAGE			
unclassified	**unclassified**	**unclassified**	**SAR**	**4**	

$$P_{ij}(\omega) = \left[e^{i\omega t_j} \frac{A^{n(j)} B^{m(j)}}{\left| \vec{r}_j - \vec{r}_t \right|} \right] \left[e^{i\omega t_i} \frac{A^{n(i)} B^{m(i)}}{\left| \vec{r}_t - \vec{r}_i \right|} \right] F(\theta_{ij}, \varphi_{ij}, \omega) P_{src}(\omega) , \quad (1)$$

where $P_{src}(\omega)$ is the frequency spectrum of the transmitted wave packet. The reflection coefficients at the upper and lower interfaces are $A(\theta_i)$ and $B(\theta_i)$. Here, θ_i simply denotes a local grazing angle at the interface, which is given by $\cos(\theta_i) = |\boldsymbol{R}_i - \boldsymbol{R}_t| / |\boldsymbol{r}_i - \boldsymbol{r}_t|$, and the *m* and *n* exponents indicate the number of interactions a ray has with a given interface. The time delay for propagation from the source to the target is $t_i = |\boldsymbol{r}_t - \boldsymbol{r}_i|$ and the delay from the target to the receiver is $t_j = |\boldsymbol{r}_j - \boldsymbol{r}_t|$. The scattering process is a convolution of a free-field scattering form function $F(\theta_{ij},\phi_{ij},\omega)$ with the incident pressure spectrum $P_{src}(\omega)$. Here, θ_{ij} and ϕ_{ij} are target-centered polar and azimuthal angles, which are related to the θ_i.

WORK COMPLETED

During FY12, the waveguide model given in (1) was reduced to a half-space model for co-located source and receiver. This model is suitable for monostatic SAS application and consists of the source and receiver locations $\boldsymbol{r}_s$ and $\boldsymbol{r}_r$ and a single image source located at $\boldsymbol{r}_{si}$ and image receiver at $\boldsymbol{r}_{ri}$. This yields four possible rays paths: S→T→R, S→B→T→R, S→T→B→R, and S→B→T→B→R, where the symbol "→" represents a propagation phase delay with S(ource), T(arget), B(ottom), and R(eceiver). The path segments S→B→T and T→B→R represent propagation from an image source to a target and from a target to an image receiver. It is noted that the first path is a direct path; the second and third paths interact with the bottom once, scatter is in a bistatic direction, and are reciprocal paths; and the last path is a backscattering path with two bottom interactions. Using $d_1 = |\boldsymbol{r}_s - \boldsymbol{r}_t|$, $d_2 = |\boldsymbol{r}_t - \boldsymbol{r}_r|$, $d_3 = |\boldsymbol{r}_{si} - \boldsymbol{r}_t|$, $d_4 = |\boldsymbol{r}_t - \boldsymbol{r}_{ri}|$, Eq. (1) reduces to

$$P(\omega) = \left[\frac{F_1(\omega)}{d_1 d_2} e^{i\omega t_1} + \frac{B(\theta_g) F_2(\omega)}{d_2 d_3} e^{i\omega t_2} + \frac{B(\theta_g) F_3(\omega)}{d_1 d_4} e^{i\omega t_3} + \frac{B^2(\theta_g) F_4(\omega)}{d_3 d_4} e^{i\omega t_4} \right] P_{src}(\omega) , \quad (2)$$

with $t_1 = (d_1 + d_2) / c$, $t_2 = (d_2 + d_3) / c$, $t_3 = (d_1 + d_4) / c$, and $t_4 = (d_3 + d_4) / c$; c being the speed of sound in water. The scattering form functions $F_k(\theta_{ij},\phi_{ij},\omega)$ in Eq. (2) depend on the locations of the sources, receivers, and target. An inverse Fouier transform of $P(\omega)$ then gives a generated sonar signal that includes the four primary acoustics paths for a target near an interface.

RESULTS

The half-space propagation model was applied to the problem of circular SAS with a target located within the CSAS path. For the results presented here, the target is placed at the center of the circular path. The target is in a broad-side orientation at 0°, 180°, and 360°. The tail of the replica is pointing at the source/receiver at 90° and the nose is pointing at the source/receiver at 270°. The radius of the path was varied from 5 to 50 m in 0.5 m increments, and adjacent signals were recorded at 1° increments along the circular path. The source and receiver were located 3.8 m above the sediment and were assumed to be omni-directional. The simulations consider the scattering from an aluminum replica of a real bullet-shaped artillery shell. The replica is ~4 inches in diamater and ~16 inches in

length with its axis of symmetry parallel to the water-sediment interface. This target was deployed during PondEx10 and finite-element model results are available for comparisons. The sound speed and density of the water are c = 1500 m/s and ρ = 1000 kg/m^3. For the simulations shown in the figures below, the sediment was considered to be an attenuating fluid. The sediment properties are c_s = 1775 m/s, ρ_s = 2000 kg/m^3, and δ = 0.008 (i.e., the loss parameter). For the simulations, the source emitted a 6 ms chirp with a carrier frequency of 16 kHz and bandwidth of 30 kHz. These parameters roughly correspond to experimental conditions during the deployment of the APL-UW's rail/tower during PondEx10. Figure 1 shows the acoustics color templates obtained from PondEx10 data, FEM simulations, and the ray-based, half-space model in SAS-ST. In Eq. (2), we use a free-field scattering form function derived from the FEM prediction of the target response where a Kirchoff-Helmholtz integral is used to propagate the scattered pressure to a 10 m range from the target. This scattered pressure is converted to a scattering form function and placed in a table: $F(\theta_i,\phi_j,\omega_k)$. Given the source and receiver locations along the circular path and the local grazing for the target location, values of θ and ϕ are determined. Linear interpolation was then employed to extract scattering form function values from the table. Inspection of Figure 1 shows that both the FEM and SAS-ST results capture much of the structure observed in the PondEx10 data. This structure includes both geometrically reflected acoustic energy and acoustic energy that couples into the elastic response of the target. Comparison of Figure 1(b) and 1(c), particularly in the −10 to −17 dB range reveals that the SAS-ST result has a slight smoothing. This is a consequence of the discrete representation of $F(\theta_i,\phi_j,\omega_k)$ and the linear interpolation.

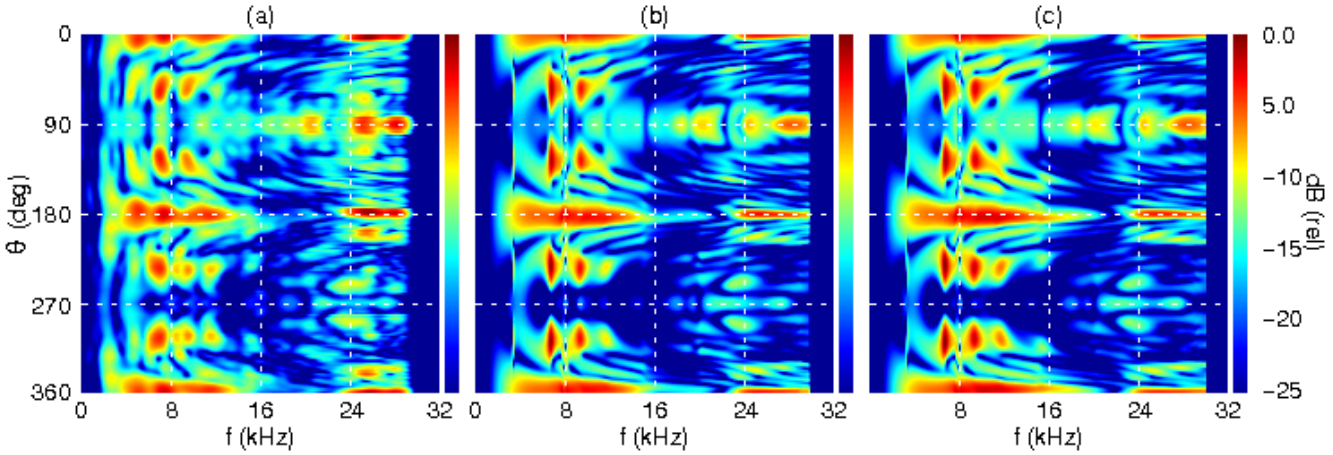

Figure 1: Acoustic color templates for an aluminum replica of a bullet-shaped artillery shell at a 10 m range. (a) PondEx10 measurement. (b) FEM and Kirchoff-Helmholtz integral result. (c) SAS-ST's ray-based, half-space model using a scattering form function derived from the scattered pressure computed in (b).

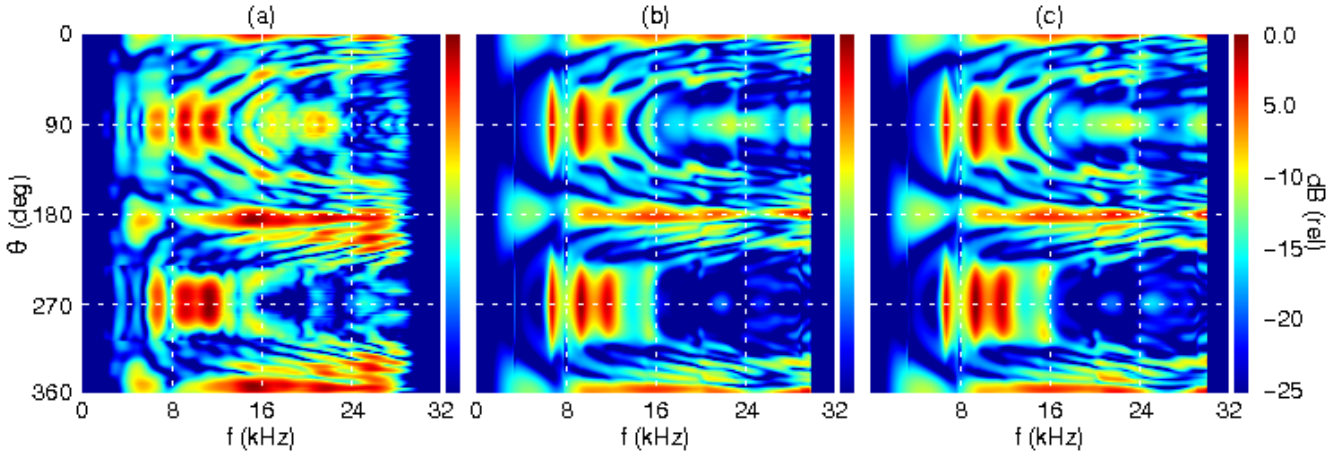

Figure 2: Acoustic color templates for an aluminum replica of a bullet-shaped artillery shell at a 5 m range. (a) PondEx10 data. (b) FEM model and Kirchoff-Helmholtz integral result. (c) SAS-ST's ray-based, half-space model.

Figure 2 shows the PondEx10 data for the aluminum replica, FEM and Kirchoff-Helmholtz integral simulation, and the SAS-ST's ray-based, half-space model for the target at a 5 m range. An important aspect of the SAS-ST simulation is that it used a $F(\theta_i,\phi_j,\omega_k)$ that was derived from a free-field FEM and Kirchoff-Helmholtz integral simulation for a target at a 10 m range. This is possible because the scattering form function is range independent and contains only the angular information and the construction of the model in Eq. (2) explicitly accounts for interactions with the water-sediment interface. Thus, only a single free-field measurement from a target or a single free-field FEM simulation is sufficent to provide a scattering form function that can be used to rapidly predict the scattering from a target near a bound at any range (provide the range meets the far field requirement).

IMPACT/APPLICATIONS

The current version of SAS-ST has been used in comparisons with data obtained during Pondex10 and Pond Experiment 2009. In addition, the new half-space model included in SAS-ST a significantly reduced computational burden (i.e., both memory and execution time) over high-fidelity FEM and Kirchoff-Helmholtz integral methods. The new half-space model permits one to investigate operational patterns in MCM scenarios such as circular SAS and can be used to generate sets of SAS signals in testing automatic target recoginition algorithm.

RELATED PROJECTS

The companion award, "Generation of Synthetic SAS Data for Targets near the Seafloor: Target Scattering Component," seeks to improve scattering models for targets near an interface used in SASSSY. The research described in the present Annual Report will be merged with the target scattering component to provide an overall improvement to the fidelity of the simulated SAS data.